RESEARCH

Synthesis of Bio-Base Fluorescence Carbon Dots for Selective Detection of Tartrazine and Sunset Yellow in Food Samples

RongGui Zhu[1] · Lei Jin[1] · Bing Yang[2] · Yuan Ma[3] · You Zhou[3] · RongDan Xiao[3] · YiJie Meng[3] · Ye Hou[3] · BenTing Xie[3] · Xiu Juan Jiang[4]

Abstract

A green, economical and simple method for the preparation of water-soluble, high-fluorescent carbon quantum dots (CQDs) has been developed via hydrothermal process using pomelo peels as carbon source. The synthesized CQDs were characterized by transmission electron microscopy (TEM), X-ray diffraction(XRD), Fourier transform infrared spectroscopy (FTIR), UV−vis absorption spectra and fluorescence spectrophotometer. The results reveal that the as-prepared C-dots were spherical shape with an average diameter of 2.64 nm and emit bright blue photoluminescence (PL) with a quantum yield of approximately 3.63%. The surface of the C-dots was rich in hydroxyl groups and presented various merits including excellent photostability, low toxicity, and satisfactory solubility. Additionally, we found that two widely used synthetic food colorants, tartrazine and sunset yellow, could result in a strong fluorescence quenching of the C-dots, The possible mechanisms are caused by different ratios of inner filter and static quenching effects. According to this property, This study attempts to establish an analytical method for the determination of tartrazine and sunset yellow using carbon quantum dots as fluorescent probe. A linear relationship was found in the range of 0-100 μM tartrazine and sunset yellow with the detection limit(3σ/k) of 0.65 nM and 1.7 nM. The relative standard deviation (RSD) was 3.5% (tartrazine) and 3.0% (sunset yellow).This observation was further successfully applied for the determination of tartrazine and sunset yellow in food samples collected from local markets, and the recovery rates of the two ranges from 79% to 117.8 and 81 -103.5%, respectively. suggesting its great potential toward food routine analysis.

Keywords Pomelo peels · Carbon quantum dots · Tartrazine · Sunset yellow · Fluorescence

Introduction

Tartrazine and sunset yellow are two types of edible synthetic pigments, which are widely used in certain food products such as beverages, candies, cakes and pastries, compound wine and dairyproducts. However, studies have shown that excessive consumption of such additives has great impact on human health [1, 2]. For example, excessive tartrazine or other artificial pigments can have toxic or adverse effects on the heart, liver, and kidneys [3, 4], and will cause ADHD in children aged 3, 8 and 9 years old [5], and can affect children's behavior and attention, too [6]. Excessive consumption of sunset yellow can cause severe allergic reactions and residual potential carcinogens [7]. For the sake of food safety, it is great significance to monitor the pigment content in food processing and production.

Until now, various instrumental techniques that analyzed pigments in foodstuff products have been increasingly employed, which include high performance liquid chromatography (HPLC)、thin-layer chromatography (TLC)Method、capillary electrophoresis、enzyme-linked immunoassay(ELISA)or spectrophotometry and electrochemical method [8]. These methods have some problems,

✉ Xiu Juan Jiang
jxjuan2010@126.com

1 College of Biological Engineering, Sichuan University of Science and Engineering, Zigong, Sichuan, China

2 Analysis and Testing Center, Dezhou University, Dezhou, Shandong, China

3 College of Chemistry and Environmental Engineering, Sichuan University of Science and Engineering, Zigong, Sichuan, China

4 College of Jia Sixie Agronomy, Weifang University of Science and Technology, Shouguang, Shandong, China

such as complex sample preparation, high operational requirements, and environmental pollution caused by the detection process. In recent years, researchers have been trying to develop new detection methods, among which CQDs detection technology has attracted much attention due to its advantages of low toxicity, good water solubility, excellent photostability, economy and simple preparation.

CQDs is generally synthesized by "Top-down" methods (laser ablation, electrochemical oxidation, etc.) and "Bottom-up" methods (combustion, hydrothermal, microwave). They are widely used in biology, materials, medicine, food and other fields [9, 10]. At present, it is crucial to develop more green methods for preparing high-quality CQDs. The use of renewable and inexpensive biomass resources can not only significantly reduce the cost of synthesizing biomass CQDs, but also reduce environmental pollution during the preparation process. Recently, hydrothermal preparation of CQDs has been reported successively by using natural substrates such as aloe vera, passion fruit shells and lentils [11].

In this study, fluorescent CQDs of pomelo peel was prepared by simple green hydrothermal method. Based on the fluorescence quenching property of CQDs, the prepared CQDs could be used as an efficient sensor for sensitive and selective determination of tartrazine and sunset yellow. The reliability of synthetic CQDs for detection was tested by measuring the concentration of tartrazine and sunset yellow in food samples from local supermarkets.

Experimental

Materials and Instruments

Chemical Reagents and Materials

Pomelo was obtained from local supermarket (Yibin, China); tartrazine ($C_{16}H_9N_4Na_3O_9S_2$,87%) and sunset yellow ($C_{16}H_{10}N_2Na_2O_7S_2$, 85%) were purchased from Aladdin Chemistry Co. Ltd. (Shanghai, China); Sodium tetraborate, mixed phosphate, potassium hydrogen phthalate were purchased from Shanghai Yidi Scientific Instrument Co. LTD (Shanghai, China); All chemicals were of analytical reagent grade and used without further purification. The ultrapure water was used throughout the experiments.

Instrumentation

UV spectroscopy detection was completed by TU1950 spectrophotometer (Persee China). The fluorescence spectra were obtained on a LS55fluorescence spectrophotometer(PerkinElmer USA), X-ray diffraction (XRD) pattern was obtained from a bruker D2 Phaser x-ray diffractometer (GER bruker). The X-ray photoelectron spectra (XPS) of CQDs were recorded by athermo fischer ESCALAB Xi+ (thermoscientific, USA). Fourier infrared spectroscopy (FTIR) was performed by Frontier FT-IR Spectrometer (PerkinElmer USA) to record the surface functional groups of CQDs, The spherical structure of CQDs were recorded by high-resolution transmission electron microscopy (Talos F200S G2, thermoscientific, USA). Fluorescent lifetime was measured by QM-8075 steady/ transient fluorescence spectrometer (Horiba, Japan).

Methods

Synthesis of Fluorescent CQDs

The preparation of CQDs in this experiment was carried out by the classic hydrothermal method: [12]fresh pomelo peels was washed and dried in the air, and then dried in an oven at 120 °C for 3 h. The dried pomelo peel was pulverized into powder by a pulverizer, and 300 mg of pomelo peel powder was added into 10 mL poly(tetrafluoroethylene)-lined autoclave with polytetrafluoroethylene, heated it at 200 °C for 6 h. After that, it was cooled and filtered with 0.22 μm filter membrane to obtain CQDs.

Sample Pretreatment

In this experiment, two kinds of candies and two kinds of beverages sold in the market were selected as test samples. The samples were purchased from a local supermarket (Yibin, China). For candy, 15 g of each sample was weighed and transferred to a centrifuge tube. 60 mL of ultrapure water was added and sonicated for about 20 min to mix thoroughly, then centrifuged at 4000 r/min for 10.0 min, and the supernatant was taken. For drinks, the preparation process was similar. All the above samples were filtered with 0.22 μm filter membrane before use.

Detection of Tartrazine and Sunset Yellow

Detection systems: the pigment detection procedure was carried out in phosphate buffer (1 M, pH 7.2) at room temperature. Different volumes of tartrazine or sunset yellow standard solution (500 μM) or sample was added into 3mL different cuvettes. Then 15 μ L CQDs was added to the above solution. After 5 min of reaction, the spectra were recorded under excitation at 330 nm with slit widths setting at 10/10 nm. All of the recoveries were calculated according to the equation below: recovery = ($C_{measured}$ − $C_{initial}$) / C_{added}.

Quantum Yield Measurements

Calculation of quantum yield of synthetic CQDs was used by the reference method [13]. Quinine sulfate solution was used as a reference standard, for which the quantum yield was 54% at 313 nm reported by the literature. The emission spectra of CQDs (ex: 330 nm) and quinine sulfate solution (10 μg/ml, Prepared by 0.05 M H_2SO_4. ex:313 nm) were measured following the previously described procedure, Their UV absorption values were determined at the same wavelengths as above. Absolute values of the quantum yield were calculated according to the equation:

$$\Phi_s = \frac{I_s}{I_{st}} \times \frac{A_{st}}{A_s} \times \left(\frac{\eta_s}{\eta_{st}}\right)^2 \times \Phi_{st}$$

where Φ was the quantum yield of the as-prepared CQDs, A was the absorbance, I was the integral area of the emission spectrum, and η was the refractive index of the solvent. The subscripts "st" and "s" referred to reference standard with known quantum yield and the CQDs solution, respectively. For the sake of reducing effects of reabsorption within the sample on the observed emission spectrum, the absorbance values (A) of all solutions were always controlled under 0.05.

Results and Discussion

Characterization of the CQDs

Figure 1 was the TEM image of the synthetic CQDs. It revealed that the CQDs were approximately spherical in shape and uniformly distributed in the solution. Particle size analysis showed that the average particle size was about 2.64 nm.

The absorption (blue line) and excitation /emission spectra (red/yellow line) of the as-synthesized CQDs were shown in Fig. 2. An obvious absorption peak was observed near 248 nm, which was caused by the π - π * transition of the C=C bond. The photoluminescent (PL) spectrum showed an optimal emission peak at about 447 nm when excited at 330 nm. The bright blue PL of the CQDs under UV light (365 nm) was strong enough to be seen with the naked eye, but when tartrazine or sunset yellow was added, the fluorescence was quenched obviously. The full width at half-maximum (fwhm) was about 80 nm, suggesting a relatively small size distribution of CQDs, which was consistent with TEM data and approximately equal to that of most reported CQDs [14, 15]. Strong fluorescence was caused generally by changes in the surface structure of CQDs.

To further investigate the optical properties, the PL emission spectra of the CQDs were recorded at progressively increasing excitation wavelengths (Fig. 3). The fluorescence intensity of the emission spectrum was the largest at the excitation wavelength of 330 nm, and the emission wavelength was unchanged basically at the excitation wavelength of 280–330 nm. But they could be observed that blue shift was attributed in the emission spectra of CQDs from 446 to
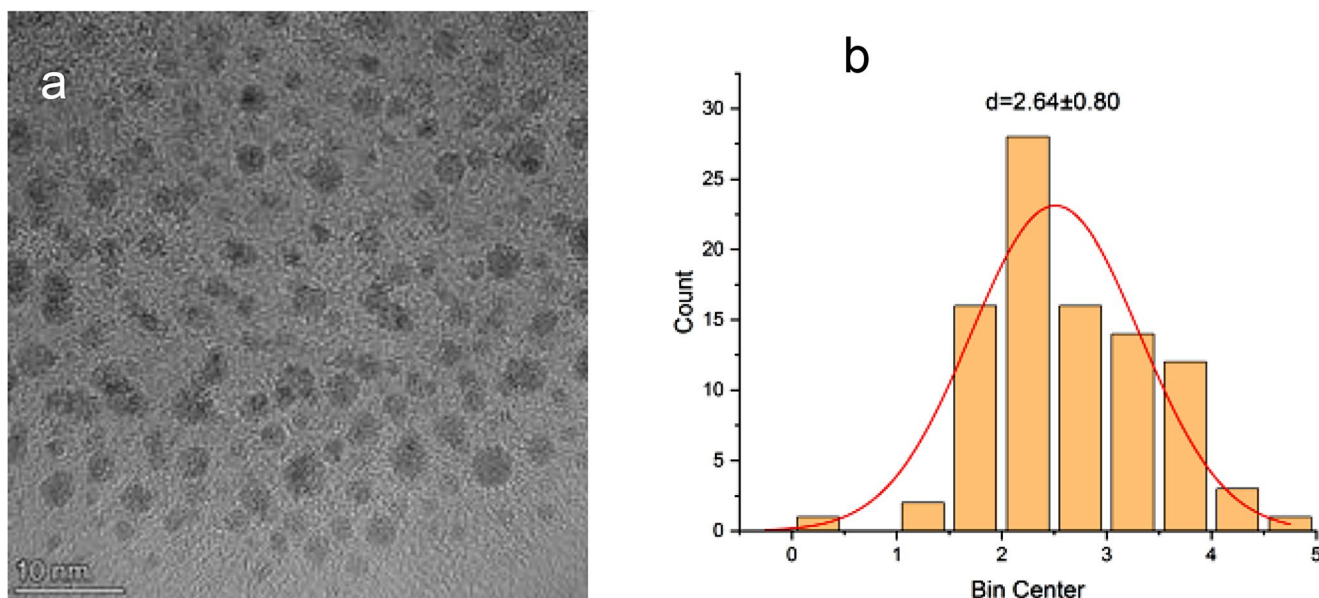

Fig. 1 TEM image of the CQDs (**a**) and the corresponding particle size distribution (**b**)

Fig. 2 UV−vis absorption (blue line), fluorescence emission (yellow line) and fluorescence excitation (red line) spectra of the CQDs. (Inset) Photographic images of CQDs under 365nm ultraviolet light (a, c), ultraviolet light with tartrazine (b) and sunset yellow (d)
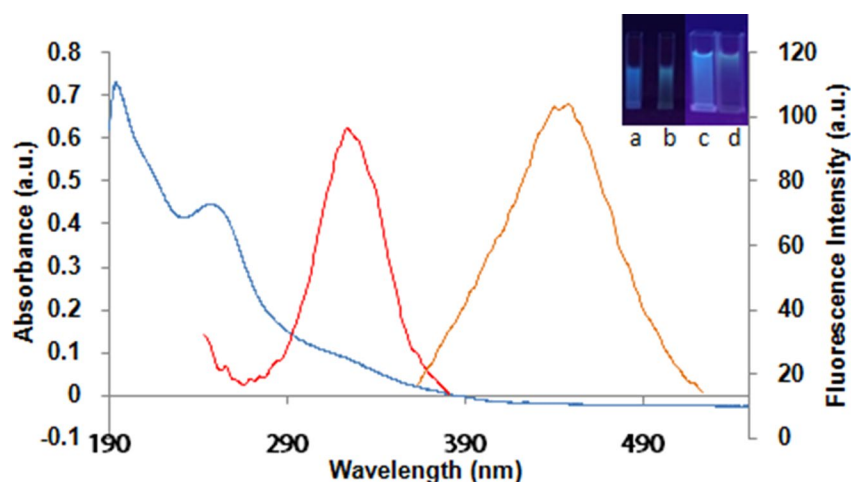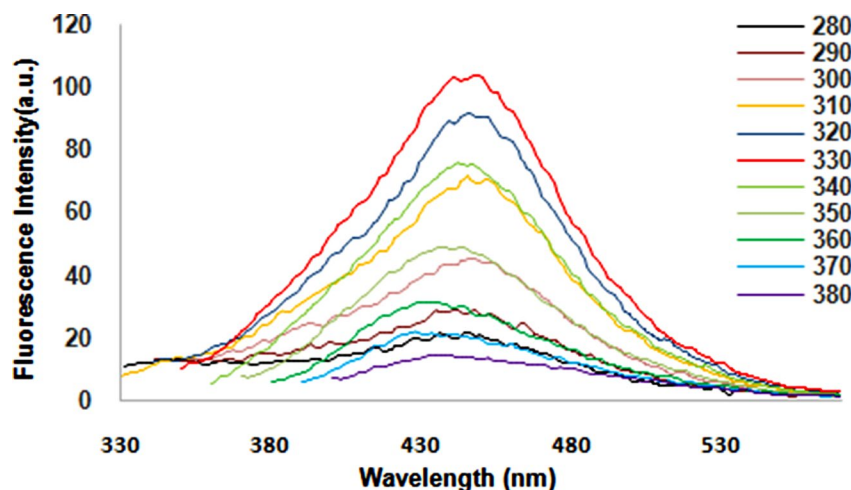
Fig. 3 Fluorescence emission spectra of CQDs obtained at different excitation wavelengths progressively increasing from 280 to 380 nm in 10 nm increments

427 nm with increasing excitation wavelengths, accompanied by a decrease of the fluorescence intensity, revealing that the fluorescence of CQDs was dependent on the excitation wavelength strongly. It was similar to the fluorescence spectral properties of some reported CQDs [16–18].

The components, surface groups and structure of the as-synthesized CQDs were further studied. As shown in Fig. 4, characteristic absorption bands of the −OH stretching vibration mode at about 3409.58 cm^{-1} and 1127.99 cm^{-1} could be observed. The band at 2929.07 cm^{-1} corresponded to the C−H stretching mode. In addition, the peaks appearing at 1604.43 cm^{-1} and 1400.29 cm^{-1} might be caused by the asymmetric and symmetric stretching vibration of COO^-, respectively. These findings demonstrated the presence of hydroxyl and carboxyl groups in pomelo peel carbohydrates.

Further the surface structure of CQDs was characterized by XPS spectroscopy. As shown in Fig. 5, there were three elements present on the CQDs: carbon (C1s, 285.3 eV), nitrogen (N1s, 400.07 eV), and oxygen (O1s, 531.95 eV) (Fig. 5A, S1), with percentages of 59.38%, 2.65%, and 37.97%, respectively. After peak splitting of the

C1s spectrum, it was found that the three main peaks were located at 284.8 eV, 286.2 eV, and 288 eV in the C1s spectrum corresponding to C-C, C-O/C-N, and C=O groups, respectively (Fig. 5B). This was consistent with the FTIR characterization results, further indicating that carboxyl groups and other functional groups could exist on the surface of CQDs. XRD showed that CQDs exhibited strong diffraction peaks around $2\theta = 31.8$ °, 45.7 °, and 56.2 ° (Fig. 5C), and slightly weaker diffraction peaks in multiple other locations. The peak patterns were relatively sharp and exhibited a certain degree of crystallinity. It was possible that nitrogen, oxygen, and CQDs had formed various combinations of new crystalline structures [19]. In addition, the relative quantum yield of synthesized CQDs was 3.63%.

Exploration of Detection Mechanism

According to relevant literature reports [20], the UV absorption spectra of tartrazine and sunset yellow exhibited strong absorption between 330 and 550 nm. Combined with the fluorescence emission spectrum and excitation spectrum analysis of CQDs in Fig. 2, there was a significant overlap
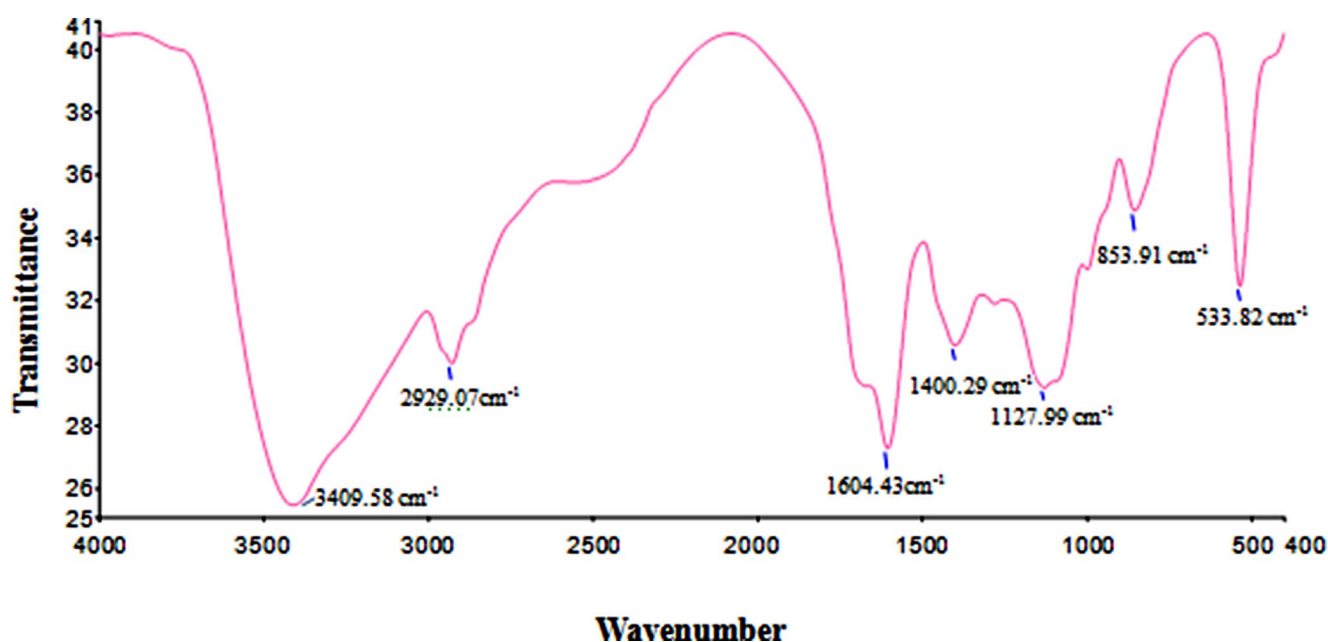
Fig. 4 FT-IR spectrum of CQDs

between the three spetra within this range, indicating that the quenching of CQDs by pigments could be caused by inner filtration effect(IFE) [21].

To further investigate the quenching mechanism, the fluorescence intensities of CQDs with increasing concentrations of the quencher were corrected according to the possible IFE, using Eq. 1 [22]:

$$F_{corr} = F_{obs} \times 10^{(Aex+Aem)/2}$$

F_{obs} and F_{corr} are the observed and corrected fluorescence intensities after excluding IFE from Fobs, respectively. Aex and Aem refer to the absorbance of the quencher at the excitation and efficiency (%E) of observed and corrected fluorescence was calculated according to Eq. 2 [23]:

$$\%E = (1 - F/F_0) \times 100\%$$

where F_0 and F refer to fluorescence emission intensities in case of absence and presence of the quencher, respectively.

The relationship between %E of observed fluorescence intensity and corrected fluorescence intensity of CQDs and pigment concentration was shown in the Fig. 6, indicating that the quenching mechanism in this study had IFE.

In addition, fluorescence quenching was usually divided into static quenching and dynamic quenching. The fluorescence lifetime of the fluorescent group did not change during static quenching, while the presence of a quenching agent in dynamic quenching led to a shortened fluorescence lifetime [24]. Fig S2 shows the fluorescence decay curves of CQDs before and after the addition of tartrazine

and sunset yellow. The fluorescence decay curves were fitted using a monoexponential function $I(t) = I_0 \exp(-t/\tau)$, where τ is the time constant of the radiative decay channel. The fluorescence lifetimes of CQDs, CQDs-tartrazine and CQDs-sunset yellow were obtained as 4.86 ns, 4.89 ns, 4.84 ns, respectively. The data showed that there was no significant change in the fluorescence lifetime of CQDs after the addition of pigments, indicating that the quenching effect of pigments on CQDs may contain static quenching.

Furthermore, dynamic quenching was generally used in the Stern-Volmer equation:

$$F_0/F = 1 + kq\tau0\,C = 1 + Ksv\,C$$

Where kq was the bimolecular quenching rate constant, $\tau0$ was the lifetime of the fluorescent chromophore before the addition of the quencher, C was the concentration of the quencher, and Ksv was the Stern-Volmer quenching constant. We used $\tau0 = 4.86 \times 10^{-9}$s calculation, obtained $kq = 4.1 \times 10^{15}$ L·mol^{-1}·s^{-1}, which was much higher than the reactive molecular diffusion constant Kdif (2.0×10^{10} L·mol^{-1}·s^{-1}). Therefore, further evidence that the quenching process could contain static quenching.

According to this characteristic of CQDs, we predicted that it was feasible to use it as a fluorescent sensor to detect this synthetic pigment in the solution simply. The synthetic method of carbon dots and its strategy of detecting pigment as a fluorescence sensor were shown in Fig. 7.
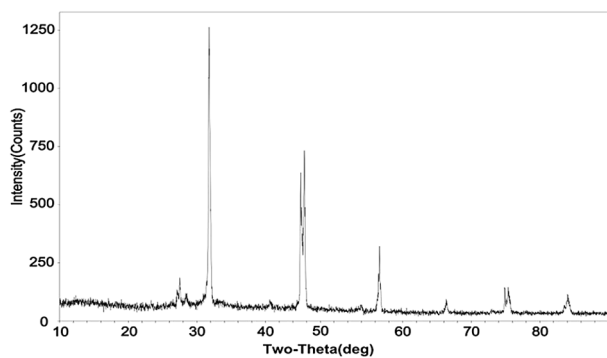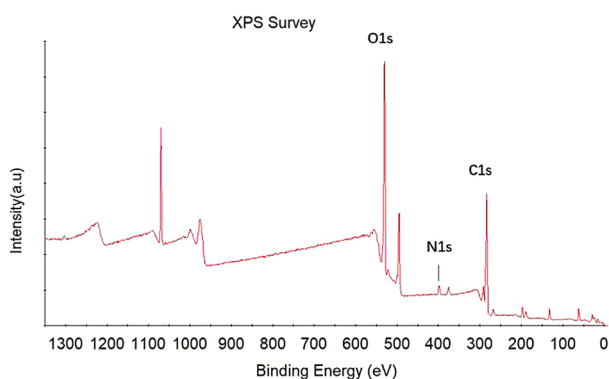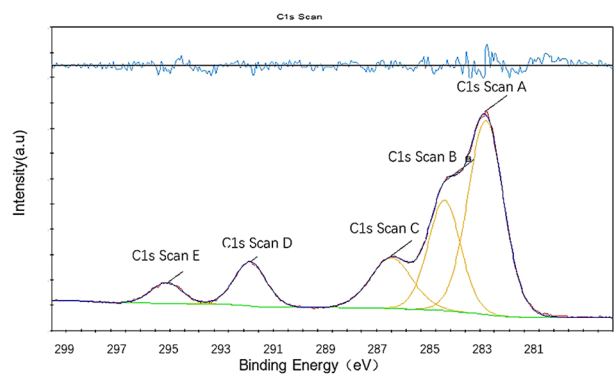
Fig. 5 Characterization of CDs obtained under **A**: XPS survey spectra; **B**: C1s survey spectra; **C**: XRD spectra

Optimization of Experimental Conditions

The fluorescence intensity changes and quenching of CQDS in different pH buffer solutions were tested and reaction time was evaluated its optimal reaction solution environment and monitoring time as a detection probe.

The effect of storage time on the fluorescence intensity of the system was shown in Fig. 8a. With the extension of storage time, the CQDs retained 97% of the fluorescence intensity during 16 days of storage at 4 °C. The fluorescence intensity did not change significantly at different storage time, its RSD was 1.3% confirming its good stability.

After adding CQDs according to the detection system described Previously, the fluorescence quenching effect changed with time as shown in Fig. 8b. The fluorescence change was basically stable within 5–30 min, with RSD of 1% (tartrazine) and 1.1% (sunset yellow), respectively. After 15 min, there is a slight decrease. In this experiment, a reaction time of 5 min was chosen.

Validation of the Developed Method

Analytical Performance for Pigments Sensing

The effect of the solution pH on the fluorescence quenching of CQDs in the presence of tartrazine and sunset yellow was shown in Fig. 8c. An increase in pH from 2.0 to 7.0 caused the increased fluorescence quenching efficiency whereas a further increase in pH from 7.0 to 13 led to a gradual decrease. Such an observation suggested that the fluorescence intensity of the CQDs strongly depended on the pH value of the system. Our results were consistent with those of CQDs functioned with hydroxyl and carboxylic/carbonyl moieties. Consequently, pH 7.2 was selected as the optimal pH.

The dependence of F_0/F on the different concentrations of tartrazine(a) and sunset yellow(b) under the identical conditions was shown in Fig. 9. As displayed, the fluorescence intensity of CQDs gradually decreased with an increase in the concentration of tartrazine and sunset yellow. As shown in the right inset of Fig. 9a and b, the change in fluorescence quenching efficiency exhibited a linear response to the tartrazine and sunset yellow concentration in the range of 0−100 μM, which was consistent with the photograph of the solutions under UV light. The calibration curve could be depicted as $F_0/F = 0.0053X + 1.0002$ and $F_0/F = 0.0032X + 1.0059$ (X was the concentration of tartrazine or sunset yellow, μM) with a correlation coefficient of 0.9921 and 0.9924.

The relative standard deviation (RSD) was 3.5% (tartrazine) and 3.0% (sunset yellow) through five parallel determinations ($n = 5$) at a fixed tartrazine concentration of 60.00 μM, indicating the excellent reliability of this sensor. The detection limit was estimated to be 0.65 nM (tartrazine) and 1.7 nM (sunset yellow) at a signal-to-noise ratio of 3.

The experimental results was compared with the reported detection methods of tartrazine and sunset yellow. As shown in Table 1, our developed assay exhibited a wider linear range

Fig. 6 Suppressed efficiency of observed and corrected fluorescence of CQDs after addition of different concentrations of tartrazine (**a**) and sunset yellow (**b**)
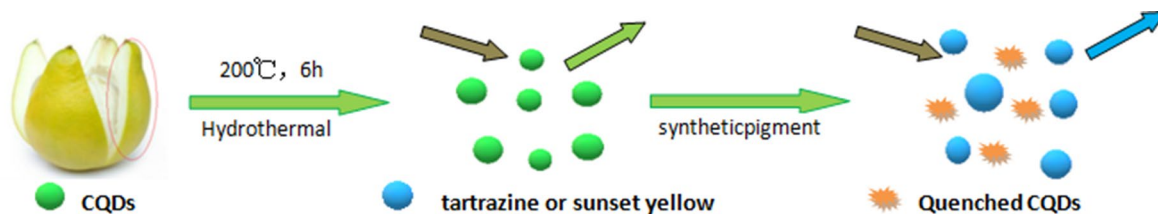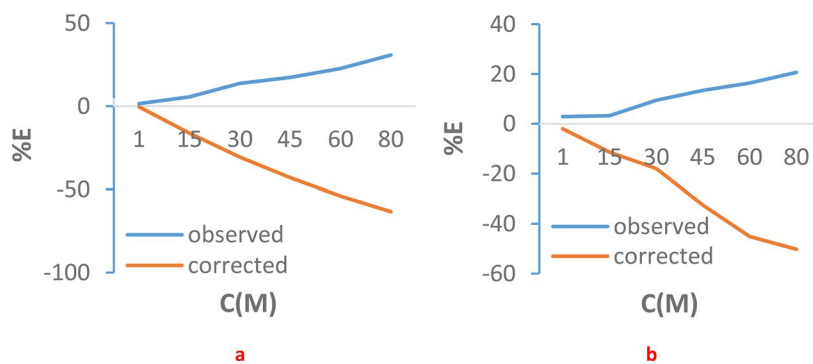

a

b

Figure 7 Scheme of the Synthetic Strategy for CQDs and the Principle of Tartrazine Sensing

Fig. 8 The effect of storage time on the fluorescence intensity of CQDs (**a**); Effect of reaction time (**b**), and pH of buffer solution (**c**) on fluorescence quenching efficiency of the C- dots − tartrazine (sunset yellow) system. F_0 and F are the intensity of CQDs in the absence and presence of tartrazine and sunset yellow, respectively. Conditions: storage temperature:4°C; PB, 1 M; tartrazine, 1.12 μM; sunset yellow, 1.13 μM
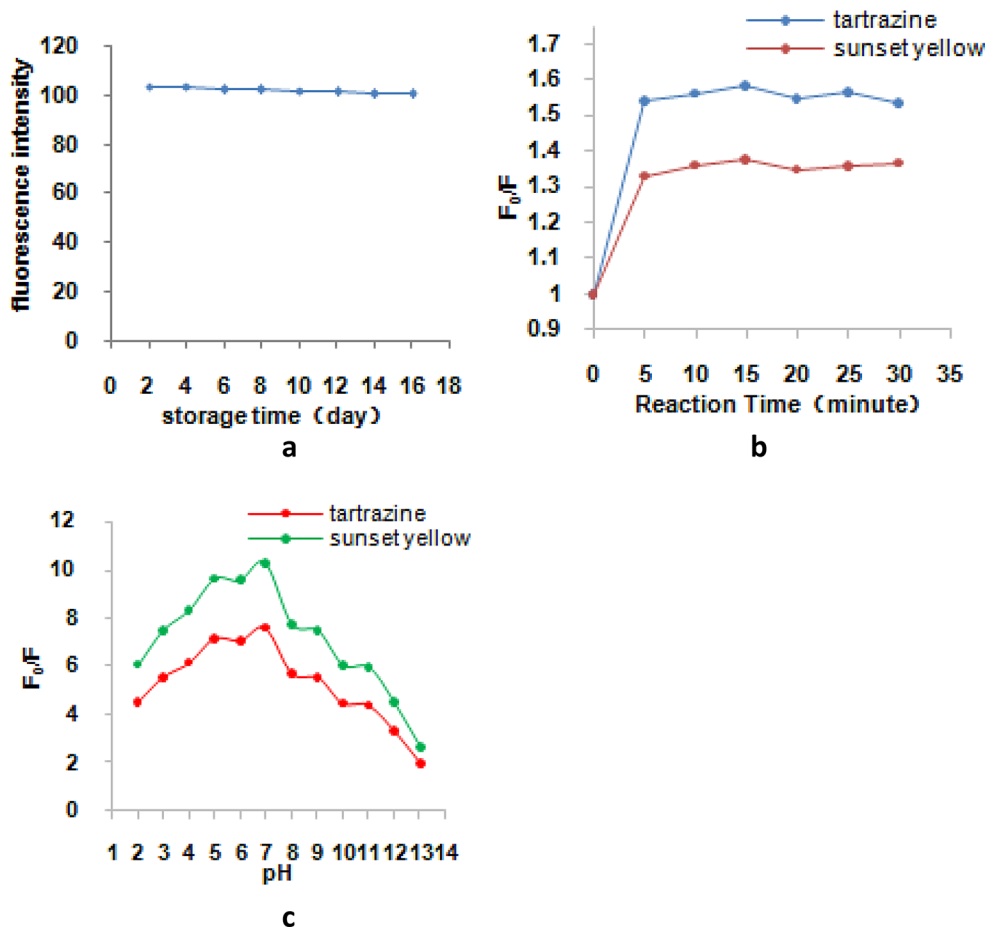

a

b

c

Fig. 9 Fluorescence emission spectra of CQDs in the presence of different concentrations of tartrazine (**a**) and sunset yellow (**b**) in 1 M PB (pH 7.2). From a to k: 0.0, 0.5, 1, 4, 7.5, 15, 30, 45, 60, 80, 100 μM, respectively. CQDs, 15 μL. (Inset) the relationship curve between F_0/F and concentration of tartrazine/ sunset yellow
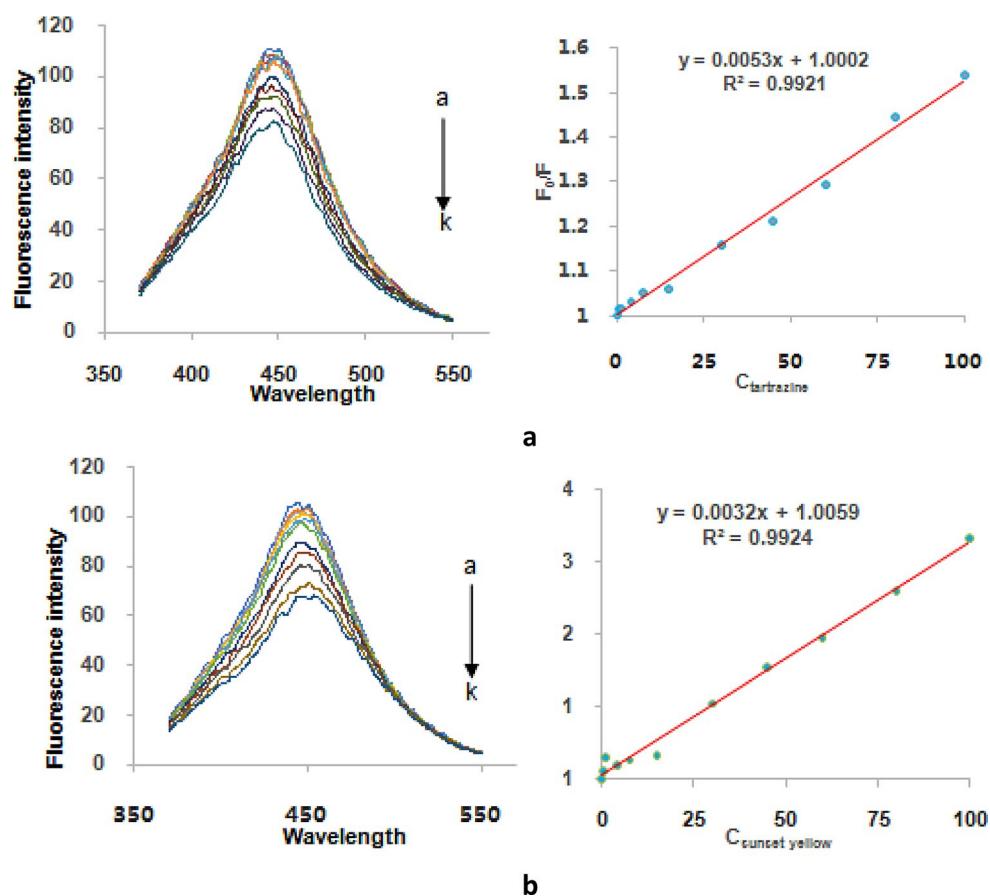

a

b

Table 1 Comparison of the proposed method with other methods for determination of pigments

Method	Pigments	Linear range (μM)	R^2	LOD (nM)	RSD%	Ref
thin-layer chromatography	tartrazine	74.9 − 356	0.992		0.03	[25]
spectrophotometry method	tartrazine	0.00131 − 0.67	0.992	0.56	0.98	[26]
high-performance liquid chromatography	tartrazine	0.0934 − 9.34	0.999	18.5	4.3	[27]
Capillary zone electrophoresis	tartrazine	5.6 − 178	0.995	2430		[28]
sulfur quantum dots	tartrazine	0.1–20	0.996	39	1.34–2.88	[29]
IL/AuTiO₂/ GO composite modified carbon paste electrode	tartrazine	1-400	0.9992	330	2.72	[30]
	tartrazine	400–1000	0.9929	330	2.72	[30]
fluorescent organic nanoparticles	tartrazine	1.5–45	0.9904	550	<5	[31]
Sensitive Electrochemical Sensor Based On an Aminated MIL-101(Cr) MOF	tartrazine	0.004-0.1	0.999	1.77	3.5	[32]
nitrogen and phosphorus co-doped carbon quantum dots	tartrazine	0.01-10	0.9962	11.6	≤3.3	[24]
Carbon Dots	tartrazine	0.25–32.5	0.9986	73	0.25	[11]
Praseodymium Doped Dysprosium Oxide-carbon Nanofibers Based Voltammetric Platform	sunset yellow	0.001–0.035	0.9952	0.312	1.5	[33]
	tartrazine	0.0015-0.04	0.9935	0.535	2.3	[33]
electrochemical sensor based on nanosheets G-C₃N₄/CPE	tartrazine	0.02-18	0.999	22	3	[34]
GO-Fe₃O₄-PAMAM and ionic liquid based electrochemical sensor	carmoisine	0.1–170	0.9998	20	3.9	[35]
fluorescence analysis	tartrazine	0.5–100	0.9921	0.65	3.5	This work
	sunset yellow	0.5–100	0.9924	1.7	3.0	

Fig. 10 Effects of potentially interfering substances: (1) cysteine; 1.7 µM; (2) copper acetate, 1.1 µM; (3) compound amino, 1.2 µM; (4) reducibility glutathion, 0.7 µM; (5) saltpeter, 2.0 µM; (6) tyrosine, 1.1 µM; (7) maltose, 0.6 µM; (8) magnesium sulfate, 1.7 µM; (9) urea, 3.3 µM; (10) potassium dihydrogen phosphate, 1.5 µM; (11) sodium citrate, 0.8 µM; (12) saccharin sodium, 0.9 µM; (13) sweet, 1.0 µM; (14) perfume, 0.7 µM; (15) vanillin, 1.3 µM; (16) sucrose, 0.6 µM; (17) histidine, 1.3 µM. Conditions: C-dots, 15 µL; PB,1 M, pH 7.2
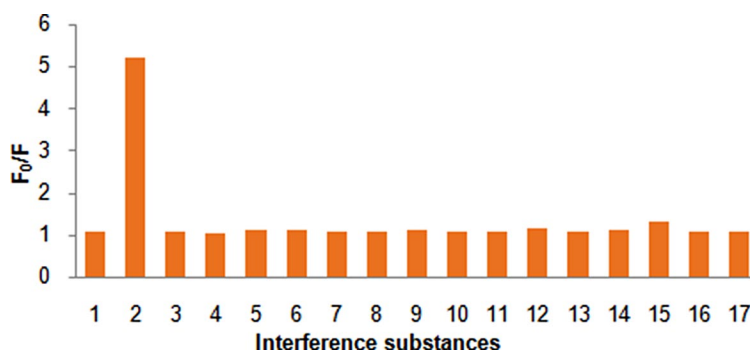

Table 2 Recovery test and precision of the analysis of tartrazine and sunset yellow in food samples

Food sample	Pigment	Detected (µM)	Spiked (µM)	Intraday			Interday		
				Found (µM)	Recovery(%)	RSD(%)	Found (µM)	Recovery	RSD(%)
Beverage(a)	tartrazine		15	11.9[b]	79.0	3.65	13.3	88.4	3.17
		0[a]	30	30.0	100.0	2.14	26.1	86.8	5.06
			60	56.4	94.0	4.13	53.7	89.6	0.51
Candy(a)	tartrazine		15	35.8	96.5	7.22	33.3	80.0	3.0
		21.3	30	52.1	102.7	4.57	46.8	85.1	5.45
			60	86.3	108.3	1.95	92.0	117.8	0.43
Beverage(b)	sunset yellow		15	23.6	88.3	3.33	22.5	81.0	4.60
		10.36	30	38.1	92.6	5.37	38.9	95.3	6.28
			60	72.3	103.3	2.96	72.2	103.0	5.42
Candy(b)	sunset yellow		15	17.8	94.3	6.15	19.2	103.5	6.0
		3.66	30	33.7	100.0	5.0	34.5	103.0	3.67
			60	62.1	97.3	2.32	61.3	96.1	3.86

a: Not detectable; b:value = mean (n = 3)

and lower limit of detection compared to other methods. Our method could be an alternative to others for the determination of tartrazine and sunset yellow in samples, although the RSD our method was not the smallest in Table 1. In addition, our CQDs had good detection performance for both tartrazine and sunset yellow, which had a wider application range and higher efficiency compared to detecting a single pigment in the table. It was worth mentioning that most of the reported sensors need special equipment, a sophisticated technique, or complicated operations. By contrast, our sensor had its own features, including low instrumentation cost, simplicity of operation, and fast response, which made it more applicable for routine analysis of tartrazine and sunset yellow in food.

The Influence of Interference Substances on Fluorescence Intensity

To evaluate the selectivity of this sensing system, we examined the fluorescence response of the system (no Pigment) with the presence of interfering substances such as cysteine, copper acetate, compound amino, reducibility glutathion, saltpeter, tyrosine, maltose, magnesium sulfate, urea, potassium dihydrogen phosphate, sodium citrate, saccharin sodium, sweet, perfume, vanillin, sucrose and histidine. The

results were shown in Fig. 10, only copper acetate in these substances caused a significant decrease in fluorescence intensity at high concentrations, but was rarely present in food. Other substances had little effect on the fluorescence intensity, and the concentration of experimental substances was much higher than those which existed in general food. So the detection method was feasible.

Application in Real Sample

To investigate the feasibility and reliability of the pigment detection method, our developed approach was employed to detect the trace level of tartrazine and sunset yellow in some food samples. The results were shown in Table 2. The intraday and interday recovery ranges of tartrazine were 79 -108.3% and 80 -117.8%, respectively, while the intraday and interday recovery ranges of sunset yellow were 88.3 -103.3% and 81 -103.5%, respectively. All of these results indicated that the accuracy and reliability of the proposed method could be applied to the determination of tartrazine and sunset yellow in food samples.

Conclusions

The new CQDs from pomelo peels was synthesized by a simple and green method. The developed method has good selectivity, sensitivity, and accuracy. At the same time, this method can detect two common pigments, reduce detection costs and time, improve the detection efficiency, and has broad application prospects in the detection of lemon yellow and sunset yellow in actual food samples. In addition, the CQDs has good potential for application in various other biotechnology development because of their excellent characteristics.

Author Contributions RongGui Zhu: investigation, data curation, formal analysis, visualization, writing – original draft.Lei Jin: investigation, formal analysis.Bing Yang: investigation, visualization. Yuan Ma, You Zhou, RongDan Xiao, YiJie Meng, Ye Hou, BenTing Xie: investigation, Xiu Juan Jiang: conceptualization, resources, writing-reviewing and editing.

Data Availability No datasets were generated or analysed during the current study.

Declarations

Ethical Approval Not applicable.

Competing Interests The authors declare no competing interests.

References

1. Silva MM, Reboredo FH, Lidon FC (2022) Food colour additives: a synoptical overview on their chemical properties, applications in food products, and health side effects. Foods. 379
2. Sambu S, Hemaram U, Murugan R, Alsofi AA (2022) Toxicological and Teratogenic Effect of Various Food Additives: An Updated Review. *BioMed Research International*. 2022
3. Salimi A, Talatappe BS, Pourahmad J (2017) Xylene induces oxidative stress and mitochondria damage in isolated human lymphocytes. Toxicol Res 33:233–238
4. Amina KA, Abdel Hameid H, Abd Elsttar AH (2010) Effect of food azo dyes tartrazine and carmoisine on biochemical parameters related to renal, hepatic function and oxidative stress biomarkers in young male rats. Food Chem Toxicol 48:2994–2999
5. McCann D, Barrett A, Cooper A, Crumpler D, Dalen L, Grimshaw K, Kitchin E, Lok K, Porteous L, Prince E, Barke ES, Warner JO, Stevenson J (2007) Food additives and hyperactive behavior in 3-year-old and 8/9-year-old children in the community: a randomized, double-blinded, placebo-controlled trial. Lancet 370:1560–1567
6. Miller MD, Steinmaus C, Golub MS, Castorina R, Thilakartne R, Bradman A, Marty MA (2022) Potential impacts of synthetic food dyes onactivity andattention inchildren: areview ofthehuman andanimal evidence. Environ Health, 2145
7. EFSA (2014) Reconsideration of the temporary ADI and refined exposure assessment for Sunset Yellow FCF (E 110). EFSA J 12:3765
8. Zhu YH, Zhao B, Wu YL (2014) Recent advances in Rapid Detection Methods of Synthetic Colorants in Foods. Hans J Food Nutr Sci 3:35–41
9. Molaei MJ (2019) Carbon quantum dots and their biomedical and therapeutic applications: a review. RSC Adv 9:6460–6481
10. Molaei MJ (2019) A review on nanostructured carbon quantum dots and their applications in biotechnology, sensors, and chemiluminescence. Talanta 196:456–478
11. Xu H, Yang XP, Li G, Zhao C, Liao XJ (2015) Green Synthesis of Fluorescent Carbon Dots for Selective Detection of Tartrazine in Food samples. J Agric Food Chem 63:6707–6714
12. Wang YQ, Luo CZ, Pan CX (2017) One-step synthesis of fluorescent carbon nanoparticles by an improved hydrothermal method. New Chem Mater 45:174–176
13. Dai HC, Shi Y, Wang YL, Sun YJ, Hu JT, Ni PJ, Li ZA Carbon dotbased biosensor for melamine detection by fluorescence resonance energy transfer. Sens Actuators B 2014,202,201 – 208
14. Meng WX, Bai X, Wang BY, Liu ZY, Lu SY, Yang B (2019) Biomass-derived Carbon dots and their applications. Energy&Environmental Mater 0:1–21
15. Cherian PKAR, Sirimahachai U, Thadathil DA, Varghese A, Hegde G Detection of picric acid in industrial effluents using multifunctional green fluorescent B/N-carbon quantum dots. J Environ Chem Eng. 2022,10,107209
16. Wan N, Wang YT, Guo TT, Yang T, Chen ML, Wang JH (2016) Green preparation of carbon dots with papaya as carbon source for effective fluorescent sensing of Iron (III) and Escherichia coli. Biosens Bioelectron 85:68–75
17. Chaudhary N, Verma D, Sharma JG, Solanki PR A novel bioinspired carbon quantum dots based optical sensor for ciprofloxacin detection. Mater Lett ,2022,308,131090.
18. Sistani S, Shekarchizadeh H Fabrication of fluorescence sensor based on molecularly imprinted polymer on amine-modified carbon quantum dots for fast and highly sensitive and selective detection of tannic acid in food samples. Anal Chim Acta ,2021,1186,339122.
19. Chen YJ, Liu ZE, Yang Q, Wang CF (2019) Zhuo. Nitrogen-doped highly photoluminescent carbon dots derived from citric acid and guanidine carbonate. J Nanosci Nanotechnol 19:4058–4063
20. Liu L, Li JQ, Guo F, Dong C (2007) Ultraviolet Spectrophotometry for simultaneous measurements of Tartrazine and Sunset yellow. Chin J Spectrosc Lab 24(3):424–427
21. Shymaa M, Abd Elhaleem F, Elsebaei S, Shalan, Belal F (2022) Utilization of N, S-doped carbon dots as a fluorescent nanosensor for determination of cromolyn based on inner filter effect: application to aqueous humour. Luminescence 37:713–721
22. Shymaa M, Abd Elhaleem F, Shalan F, Belal, Elsebaei F (2022) Insights for applying N, S-doped carbon dots as a fluorescent nanoprobe for estimation of some nitro-calcium channel blockers. Royal Soc Open Sci 9:220609
23. Shymaa M, Abd Elhaleem F, Elsebaei S, Shalan, Belal F (2022) Turn-off fluorescence of nitrogen and sulfur carbon quantum dots as effective fluorescent probes for determination of imatinib. Application to biological fluids. *Spectrochimica Acta Part A: Molecular and Biomolecular Spectroscopy*, 272,120954
24. Liu LF, Sun HJ, Cui YK, Yang ZQ, Xiao LX (2022) Fluorescence probe based on nitrogenand phosphorus co-doped carbon

quantum dots for tartrazine detection in food stuffs. Chem Res Application 34:188–198

25. Soponar F (2008) Mot and *C.Sǎrbu*, quantitative determination of ˘some food dyes using digital processing of images obtained by thinlayer chromatography. J Chromatogr A 1188:295–300

26. Hsu PC, Shih ZH, Lee CH, Chang HT (2012) Synthesis and analytical applications of photoluminescent carbon nanodots. Green Chem 14:917–920

27. Li WJ, Zhou X, Tong SS, Jia Q (2013) Poly (Nisopropylacrylamide-co-N,N′-methylene bisacrylamide) monolithic column embedded with g-alumina nanoparticles microextraction coupled with high-performance liquid chromatography for the determination of synthetic food dyes in soft drink samples. Talanta 105:386–392

28. Pérez-Urquiza M, Beltrán JL (2000) Determination of dyes in ˊ foodstuffs by capillary zone electrophoresis. J Chromatogr A 898:271–275

29. Peng XH, Wang Y, Wang QY, Tang JJ, Zhang MS, Yang XP Selective and sensitive detection of tartrazine in beverages by sulfur quantum dots with high fluorescence quantum yield. Spectrochimica Acta Part A: Mol Biomol Sectroscopy. 279,2022,121454

30. State RG, Staden JF, State RN, Papa F (2022) Rapid and sensitive electrochemical determination oftartrazinein commercial food samples using IL/AuTiO2/GO composite modified carbon paste electrode. Food Chem 385:132616

31. Lin LP, Zheng QL, Chen QH, Fang M, Lai QJ, He XH, Qin JY, Zu J, Lin ZJ, Lin RG (2022) Preparation of fluorescent organic nanoparticlesvia self-polymerization for tartrazine detectionin food samples. New J Chem 46:4756–4761

32. Massah RT, Jiokeng SLZ, Liang J, Njanja E, MNtep TM, Spiess A, Rademacher L, Janiak C, Tonle IK (2022) Sensitive Electrochemical Sensor based on an aminated MIL-101(cr)MOF for the detection of Tartrazine. ACS Omega 7:19420–19427

33. Baytak AK, Aslanoglu M (2022) Praseodymium doped Dysprosium Oxide-carbon nanofibers based voltammetric platform for the simultaneous determination of Sunset Yellow and Tartrazine. Electroanalysis 34:1–14

34. Marahel F, Niknam L (2022) Application electrochemical sensor based onnanosheets G-C3N4/CPE by square-wave anodicstripping voltammetric for measure amounts of toxic tartrazine color residual in different drinkand foodstuffs. J Environ Sci Health Part B 57:489–496

35. Nejad FG, Sheikhshoaie I, Beitollahi H (2022) Simultaneous detection of carmoisine and tartrazine in food samples using GO-Fe3O4-PAMAM and ionic liquid based electrochemical sensor. Food Chem Toxicol 162:112864